EDGEWOOD CHEMICAL BIOLOGICAL CENTER
U.S. ARMY RESEARCH, DEVELOPMENT AND ENGINEERING COMMAND
Aberdeen Proving Ground, MD 21010-5424

ECBC-TR-1231

PLATFORM APPROACH TO PRODUCE POLYMER NANOPARTICLES WITH MODULAR FUNCTIONALITY FROM AMPHIPHILIC BLOCK COPOLYMER STABILIZERS

Kato L. Killops

RESEARCH AND TECHNOLOGY DIRECTORATE

Christina Rodriguez
Nathaniel A. Lynd

MATERIALS RESEARCH LABORATORY
UNIVERSITY OF CALIFORNIA, SANTA BARBARA
Santa Barbara, CA 93106-5121

April 2014

Disclaimer

The findings in this report are not to be construed as an official Department of the Army position unless so designated by other authorizing documents.

REPORT DOCUMENTATION PAGE

Form Approved
OMB No. 0704-0188

1. REPORT DATE *(DD-MM-YYYY)*	2. REPORT TYPE	3. DATES COVERED *(From - To)*
XX-04-2013	Final	Mar 2012 - Dec 2013

4. TITLE AND SUBTITLE
Platform Approach to Produce Polymer Nanoparticles with Modular Functionality from Amphiphilic Block Copolymer Stabilizers

5a. CONTRACT NUMBER

5b. GRANT NUMBER

5c. PROGRAM ELEMENT NUMBER

6. AUTHOR(S)
Killops, Kato L. (ECBC); Rodriguez, Christina; Lynd, Nathaniel A. (MRL UCSB)

5d. PROJECT NUMBER

5e. TASK NUMBER

5f. WORK UNIT NUMBER

7. PERFORMING ORGANIZATION NAME(S) AND ADDRESS(ES)
Director, ECBC, ATTN: RDCB-DRP-F, APG, MD 21010-5424
Material Research Laboratory, MC 5121 University of California, Santa Barbara, CA 93106-5121

8. PERFORMING ORGANIZATION REPORT NUMBER
ECBC-TR-1231

9. SPONSORING / MONITORING AGENCY NAME(S) AND ADDRESS(ES)

10. SPONSOR/MONITOR'S ACRONYM(S)

11. SPONSOR/MONITOR'S REPORT NUMBER(S)

12. DISTRIBUTION / AVAILABILITY STATEMENT
Approved for public release; distribution is unlimited.

13. SUPPLEMENTARY NOTES

14. ABSTRACT:
Polymer nanoparticles with peripheral functionality were synthesized via emulsion polymerization using an amphiphilic block copolymer (BCP) surfactant. The polystyrene-*block*-poly(ethylene oxide-*co*-allyl glycidyl ether) BCPs with various lengths and functional monomer incorporation were synthesized using anionic polymerization. Modification of the allyl groups was achieved by thiol-ene chemistry using commercially available mercaptans. Particles ranged in size from <100 nm to just >200 nm. Functionalized particles exhibited pH modulation as monitored by electrophoretic mobility measurements.

15. SUBJECT TERMS
Nanoparticle, Latex, Polystyrene, Block copolymer, Zeta potential, Thiol-ene, Colloid

16. SECURITY CLASSIFICATION OF:			17. LIMITATION OF ABSTRACT	18. NUMBER OF PAGES	19a. NAME OF RESPONSIBLE PERSON
a. REPORT	b. ABSTRACT	c. THIS PAGE			Renu B. Rastogi
U	U	U	UU	30	19b. TELEPHONE NUMBER *(include area code)* (410) 436-7545

Blank

PREFACE

The work described in this report was authorized under the Army In-house Laboratory Independent Research program. The work was started in March 2012 and completed in December 2013.

The use of either trade or manufacturers' names in this report does not constitute an official endorsement of any commercial products. This report may not be cited for purposes of advertisement.

This report has been approved for public release.

Acknowledgments

The authors acknowledge Erica R. Valdes for her support of this program through scanning electron microscope image collection and instrument operation.

Blank

CONTENTS

FIGURES

TABLES

PLATFORM APPROACH TO PRODUCE POLYMER NANOPARTICLES WITH MODULAR FUNCTIONALITY FROM AMPHIPHILIC BLOCK COPOLYMER STABILIZERS

1. INTRODUCTION

The ability to synthesize colloidal polymer particles in the nanoscale size regime with tunable peripheral functionality has attracted much attention in recent years. Emulsion or dispersion polymerization techniques are often used to achieve spherical particles. Emulsion polymerization techniques are highly amenable to industrial processes because of the ease of scalability and use of water as the solvent. Tailoring the functionality of a particle lies at the nexus of advanced purification strategies,[1,2] as well as expanding opportunities for phonic materials,[3] smart coatings,[4,5] and abiotic-biological interfaces.[6,7]

Many strategies exist for achieving functional polymer colloids. Mixing a range of monomers in desired proportions can lead to particles with diverse functionality via precipitation polymerization.[7,8] Statistically, these monomers should be observed on the particle surface, especially if charged or hydrophilic monomers are used.[9] Within the realm of emulsion polymerization, common approaches include incorporation of reactive surfactants or surfmers[10] (surfactant monomers) to achieve peripheral functionality. An alternative approach is to use amphiphilic block copolymers (BCPs) to stabilize emulsion particles,[11] resulting in latexes with a polymer corona. Although a number of different BCPs have been used, polystyrene-*b*-poly(ethylene oxide) (PS-*b*-PEO) has been widely studied in emulsion polymerizations.[12–14] However, PS-*b*-PEO lacks the capacity to be further modified or functionalized.

The use of BCP stabilizers offers a number of advantages over their small molecule counterparts, including low critical micelle concentrations and low diffusion coefficients, which aid in anchoring the macromolecules to the particle interface.[15] Our approach capitalizes on the opportunity for macromolecules to provide *multiple* modular functional groups on a single stabilizer molecule. Furthermore, the advantage of using a BCP *platform* is that a single precursor polymer can be modified with a variety of functional groups in order to create a library of functional particles.

Herein, we describe the synthesis of polystyrene (PS)-based latexes with tunable peripheral functionality by starting from a PS-*b*-poly(ethylene oxide [EO]-*co*-allyl glycidyl ether]) (PS-*b*-P[EO-*co*-AGE) amphiphilic BCP.[16–17] The incorporation of an allyl-functional monomer into the hydrophilic portion of the BCP enables the use of thiol-ene "click" chemistry[18] to decorate the polymer backbone with a diverse range of commercially available thiol functional groups (Figure 1). This platform approach enables the modification of allyl groups with a variety of moieties that are charged or neutral, pH sensitive, and zwitterionic. In this report, we determine how a number of parameters affect particle formation and stabilization, including BCP molecular weight, BCP composition, BCP incorporation in emulsion polymerization, and type and charge of functional groups within the BCP.

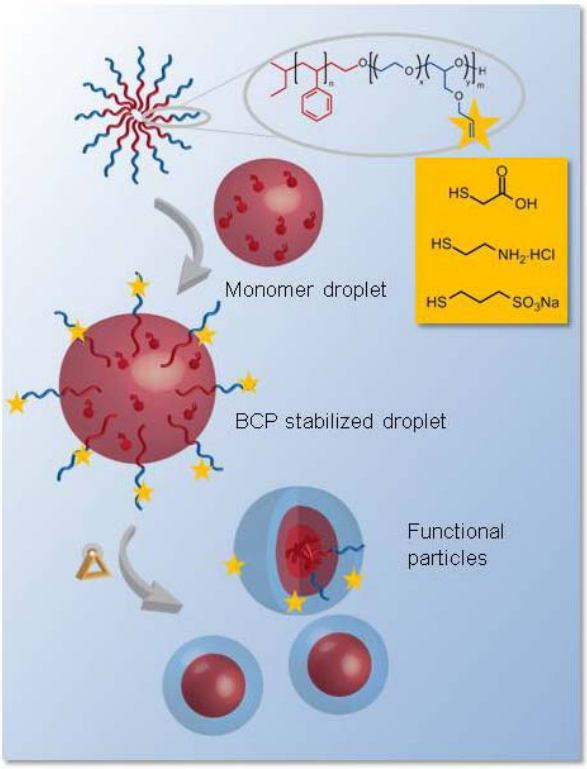

Figure 1. Schematic representation of using emulsion polymerization with modular BCP stabilizers to produce latexes with functional corona.

2. EXPERIMENTAL PROCEDURES

2.1 Chemicals

All chemicals were purchased from Sigma Aldrich (Saint Louis, MO) and used without further purification, unless otherwise stated. Allyl glycidyl ether (AGE) was purchased from TCI America (Portland, OR). Styrene was degassed using three freeze-pump-thaw cycles and purified by stirring over dibutylmagnesium at 0 °C and distilling into receiving flasks. EO and AGE were degassed using three freeze-pump-thaw cycles, purified by stirring over butylmagnesium chloride at 0 °C, and distilled into receiving flasks. Deuterated solvents for nuclear magnetic resonance (NMR) were purchased from Cambridge Isotope Laboratories (Tewksbury, MA). Potassium naphthalenide was prepared by dissolving recrystallized naphthalene (10 g) in dry tetrahydrofuran (THF [250 mL]) and then adding potassium metal (3 g) under positive argon pressure. The system was closed with a septum and allowed to stir overnight, which yielded a dark green solution of 0.3 M potassium naphthalenide. Basic aluminum oxide was used to remove the inhibitor present in the styrene monomer prior to emulsion polymerization.

2.2 Instrumentation

NMR (^{1}H,^{13}C) spectra were recorded on a Bruker DMX-300 MHz (Billerica, MA) spectrometer at room temperature. Chemical shifts are reported in parts per million (δ) relative to chloroform (7.24 ppm for ^{1}H), dimethyl sulfoxide (DMSO [2.50 ppm for ^{1}H]), or dimethylformamide (DMF [8.03 ppm for ^{1}H]) as an internal reference. Gel permeation chromatography was performed in chloroform with 0.25% triethylamine on a Waters 2695 separation module (Milford, MA) equipped with a Waters 2414 refractive index detector and a Waters 2996 photodiode array detector. X-ray photoelectron spectroscopy (XPS) measurements were performed using a Kratos Axis ultra spectrometer (Kratos Analytical, Manchester, UK) with a monochromatic Al Kα X-ray source (1486.6 eV) operating at 225 W under a vacuum of 1.0×10^{-8} Torr. Charge compensation was carried out by injection of low-energy electrons into the magnetic lens of the electron spectrometer. The pass energy of the analyzer was set at 80 eV for survey scans with a resolution of 0.5 eV. The spectra were analyzed using CasaXPS v.2.3.14 software (Cheshire, UK). The C–C peak at 285 eV was used as the reference for binding energy calibration. Scanning electron microscopy (SEM) was performed on a FEI XL30 Sirion FEG digital electron scanning microscope (Hillsboro, OR) at 3.0 to 5.0 keV. Dynamic light-scattering (DLS) and zeta-potential measurements were performed on a Wyatt Mobius (Santa Barbara, CA) instrument at ambient temperature in Milli-Q water (EMD Millipore, Billerica, MA). BCP and latex samples were diluted and filtered through a 1.6 μm glass filter before DLS measurement was performed.

2.3 Synthesis

PS-*b*-P(EO-*co*-AGE) (PS-b-P(EO-co-AGE)) synthesis was performed according to procedures reported by Killops et al.[19]

2.3.1 Functionalization of PS-*b*-P(EO-*co*-AGE) via Thiol-ene Chemistry

Polymer was dissolved in a minimal amount of solvent (typically DMF or THF) in a vial fitted with a septum, and ca. 10 eq. (relative to ene) of thiol, and 0.2 eq. (relative to ene) 2,2-dimethoxy-2-phenylacetophenone were added. The mixture was sparged with nitrogen for 5 min before the vial was irradiated with 365 nm light for 30 min. Conversion of the ene groups was verified by ^{1}H NMR. Functionalized polymers were purified using dialysis against Milli-Q water for 24 h to remove unreacted thiol and lyophilized to dry.

2.3.2 Particle syntheses

A general recipe was used and scaled accordingly: 10 wt % styrene in water, 5–20 wt % BCP (relative to styrene), and 0.8 wt % (relative to styrene) potassium persulfate. Reactions were conducted in 25 to 100 mL of water. First, styrene was suspended with vigorous stirring in half of the total volume of water in a three-neck flask fitted with a condenser. The BCP was dissolved in the other half of the water. The BCP-micelle solution was added dropwise to the stirring styrene suspension. The mixture was sparged with nitrogen gas for 30 min at room temperature and then heated to 80 °C under nitrogen gas flow. In a separate vial fitted with a septum, potassium persulfate was dissolved in a small amount of water and sparged with

nitrogen gas for 10 min. The solution was transferred via cannula to the reaction mixture. The emulsion polymerization was stirred at 80 °C for 6–16 h.

3. RESULTS AND DISCUSSION

3.1 BCP Syntheses

To create a platform to synthesize polymer nanoparticles with diverse peripheral functionality, an amphiphilic BCP scaffold was devised to serve as an emulsion polymerization stabilizer. The PS-*b*-P(EO-*co*-AGE) BCP contained a PS block to anchor the BCP to the particle and a hydrophilic EO-based block to stabilize the styrene droplets in the aqueous reaction medium. Within the EO block, allyl groups were dispersed along the backbone via copolymerization with AGE, which permitted pre- or post-polymerization functionalization with a range of hydrophilic thiol groups. The PS-*b*-P(EO-*co*-AGE) BCPs were synthesized via standard anionic polymerization[19] in large (>10 g) quantities, starting from a PS macroinitiator.

A range of PS-*b*-P(EO-*co*-AGE) BCPs were synthesized in order to ascertain the effect of molecular weight and AGE incorporation on particle formation, and they were characterized by size-exclusion chromatography (SEC) and ^{1}H NMR. As shown in Table 1, the molecular weights of both the hydrophobic and hydrophilic blocks were varied. Incorporation of AGE monomer ranged from 1 to 5 mol%, relative to EO. Because the relative weight percentages of the hydrophilic and hydrophobic blocks are of critical importance to emulsion stabilization,[20] hydrophilic block weight percentages for all BCPs are in the range of 75 to 85 wt%. Furthermore, the calculated hydrophilic-lipophilic balance (HLB) for each polymer resides in the range of 14–16. HLB values greater than 12 are predicted to stabilize oil-in-water emulsions.[21]

Table 1. Synthesized BCPs

Polymer Group	Naming Convention	M_n[a] PS[b] (Da)	M_n PEO[c] (Da)	M_n PAGE[c] (Da)	Mol % AGE	Total M_n (Da)	PDI[d]
PS_5-P(EO-*co*-AGE)$_{15}$	**S3**	5,000	14,100	900	3	20,000	1.08
	M1	11,000	49,100	1,100	1	61,200	1.05
PS_{11}-P(EO-*co*-AGE)$_{50}$	**M3**	11,000	42,400	3,200	3	56,600	1.04
	M5	11,000	44,200	6,600	5	61,800	1.06
PS_{16}-P(EO-*co*-AGE)$_{90}$	**L3**	16,000	82,000	6,000	3	104,000	1.09

[a] Number average molecular weight
[b] Determined by SEC
[c] Determined by NMR
[d] Poldispersity index

3.2 BCP Micelles

Aqueous solutions of BCPs were prepared in order to investigate micelle size and aggregation. Concentrations of 0.1 and 0.5 mg/mL, well above the critical micelle concentration for PS-*b*-PEO systems,[22] were evaluated using DLS. For each of the five polymers, there exists a multimodal population of structures, which is well documented in the literature for PS-*b*-PEO micelles.[23–26] Using light scattering studies, Xu et al. found that irrespective of concentration, micelles (ca. R_h 20 nm) and micellar clusters (ca. R_h 70 nm) coexist.[23] Windzor and coworkers also observed a bimodal distribution of PS-*b*-PEO structures at a range of molecular weights, with micelles of ca. 20–40 nm and aggregates of ca. 135–200 nm in diameter.[25] Here, we observed two to three populations of micelle structures (shown in Table 2). The size of the structures observed did not correlate with the molecular weights of the BCPs. We believe that the populations consist of free unimer BCP (R_1),[26] micelles (R_2), and micelle aggregates (R_3).

Table 2. Radii of BCP Micelle Structures from DLS

	0.1 mg/mL BCP			**0.5 mg/mL BCP**		
Polymer	R_1	R_2	R_3	R_1	R_2	R_3
S3	6 ± 1	68 ± 7	214 ± 20	4 ± 0	46 ± 5	126 ± 8
M1	–	61 ± 4	140 ± 16	9 ± 1	89 ± 11	271 ± 25
M3	8 ± 1	53 ± 6	138 ± 16		40 ± 1	136 ± 15
M5	–	38 ± 2	129 ± 6		49 ± 0	176 ± 20
L3	6 ± 1	96 ± 9	217 ± 23	6 ± 0	31 ± 4	138 ± 23

Size determined using Dynamics software from Wyatt Technology Corporation (Santa Barbara, CA).
R_1, R_2, and R_3 include structures of 1–10, 10–50, and 50–200 nm, respectively.

3.3 Emulsion Polymerization

Emulsion polymerizations were carried out in large batches with water, styrene, potassium persulfate, and PS-*b*-P(EO-*co*-AGE) as the only emulsion stabilizer. Initially, alkene functional particles were prepared using BCP **M1**. Particle size was determined using SEM and DLS (Table 3). The diameters of particles containing BCP measured using DLS were consistently larger than those measured with SEM. Measurements using DLS included the hydrodynamic diameter of the solvated corona, whereas that layer collapsed in SEM.

We observed that the amount of BCP stabilizer had a substantial effect on the final diameter of the particles for polymer **M1**. A marked decrease in diameter was observed upon increasing the **M1** content from 10 to 15 wt%. However, upon increasing the BCP content from 15 to 20 wt%, a saturation point was reached, where steric crowding of the chains prevented additional stabilization of smaller particles.[27] Similarly, particles synthesized using **M3** were larger and polydispersed at 5 wt%, but they decreased in size and polydispersity when

the concentration of BCP was increased to ≥10 wt%. Others have found that both reaction rate and final particle size were closely correlated to the concentration of PS-*b*-PEO in the emulsion polymerization.[12, 14, 28] To determine the effect of molecular weight on particle formation in this system, our BCP library was expanded to include BCPs consisting of smaller (**S3**) and larger (**L3**) molecular weights relative to **M3**, while keeping the fraction of PS near 20 wt%.

Table 3. Average Diameters of Particles with Varying BCP Content

BCP Used	Wt% BCP	D_{DLS}[a] (nm)	D_{SEM}[b] (nm)
None	0	265 ± 0	280 ± 13
S3	10	82 ± 5	55 ± 2
S3	15	93 ± 2	62 ± 3
S3	20	78 ± 2	86 ± 4
M1	10	122 ± 5	100 ± 4
M1	15	114 ± 9	80 ± 2
M1	20	107 ± 6	77 ± 1
M3	5	166 ± 12	185 ± 71
M3	10	101 ± 4	72 ± 3
M3	15	103 ± 1	75 ± 4
M3	20	119 ± 3	74 ± 4
M5	10	–	Too polydisperse
L3	10	173 ± 5	141 ± 7
L3	15	142 ± 3	110 ± 3
L3	20	128 ± 7	82 ± 13

[a] Determined using DLS using Wyatt Dynamics software.
[b] Determined by SEM using ImageJ software (National Institutes of Health, Bethesda, MD).

Figure 2 shows representative SEM images of particles formed at a range of BCP concentrations from BCPs of varying molecular weight and AGE incorporation. Particles formed from **M1** and **M3** were relatively monodispersed, and showed a decrease in particle size with increasing BCP incorporation.[14] These particles had low polydispersity, and had a propensity to crystallize into iridescent colloidal arrays. This trend was not repeated in the case of **S3** and **L3**, where the polydispersity increased, and particle diameter was not correlated to BCP incorporation. For **S3**, the size of the particles actually increased with increasing BCP content, which was likely because of the availability of more chains so larger monomer droplets could be stabilized against coalescence without the steric effects that hindered the packing of larger BCPs into droplets.[25] In the case of **L3**, the number of chains available for stabilization was lower, leading to increasing polydispersity. Furthermore, polydispersity may also have been influenced by decreases in the diffusion coefficient of larger BCPs, which caused them to become entrapped

within the particles more easily, where they were unavailable to stabilize the interface.[12] The number of particles (N_p) was also found to be dependent on BCP concentration (Figure 3).[13,28] At higher [BCP], more micelles were available for nucleation and a larger number of particles could be stabilized.[15]

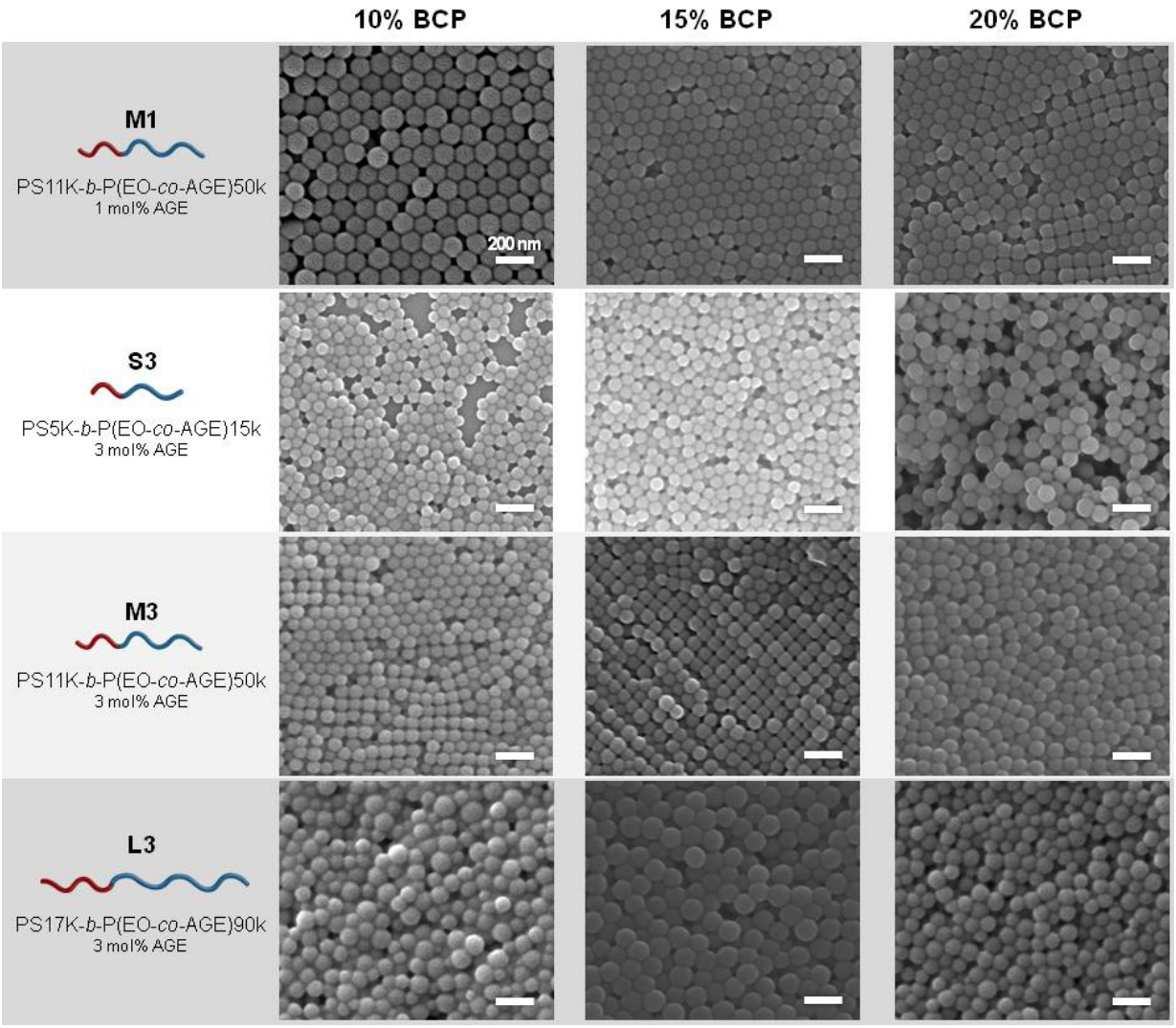

Figure 2. SEM images of particles synthesized with different BCP stabilizers and varying incorporations of BCP stabilizer. All scale bars are 200 nm.

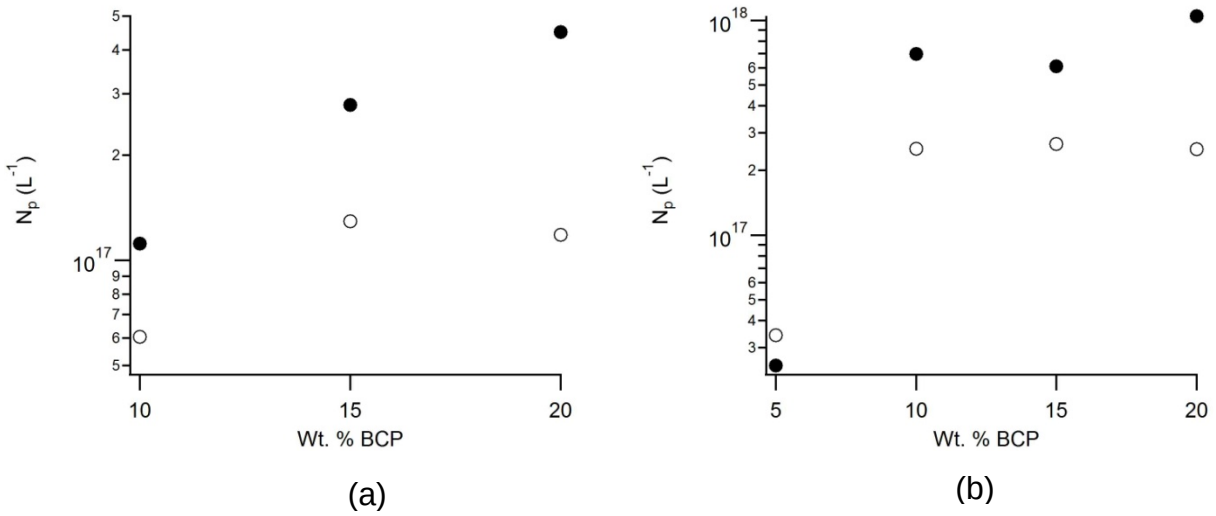

Figure 3. Plots of number of particles (N_p) vs wt% BCP for (a) **L3** and (b) **M3**.

To gain further insight into the mechanism of particle formation, a time sweep of the polymerization was conducted by removing an aliquot from the reaction and quenching it with radical inhibitor. Particle formation was monitored using DLS (data presented in Figure 4). In the time sweep of **S3**, three size populations were observed after filtering the solution through a 1.6 μm filter. Before polymerization, BCP unimers (ca. 5 nm radius) and micelle aggregates (ca. 40 nm radius) were observed. It is possible that the population at ca. 40 nm contained both micelles and aggregates that could not be resolved. As the polymerization began, large structures were observed as well (ca. 400 nm radius). We believe that these were monomer droplets, which acted as monomer reservoirs and were depleted over the course of the reaction because they were not observed after 4 h. In work by Winzor et al., the authors observed PS-*b*-PEO micellar aggregates, which retained their size upon swelling by monomer.[25] We observed a comparable phenomenon, where the particles at the end of polymerization were of a size similar to that of the initial micelle aggregate. The DLS measurements indicated that this polymerization of **S3** at 15 wt% BCP incorporation yielded particles of ca. 100 nm in diameter.

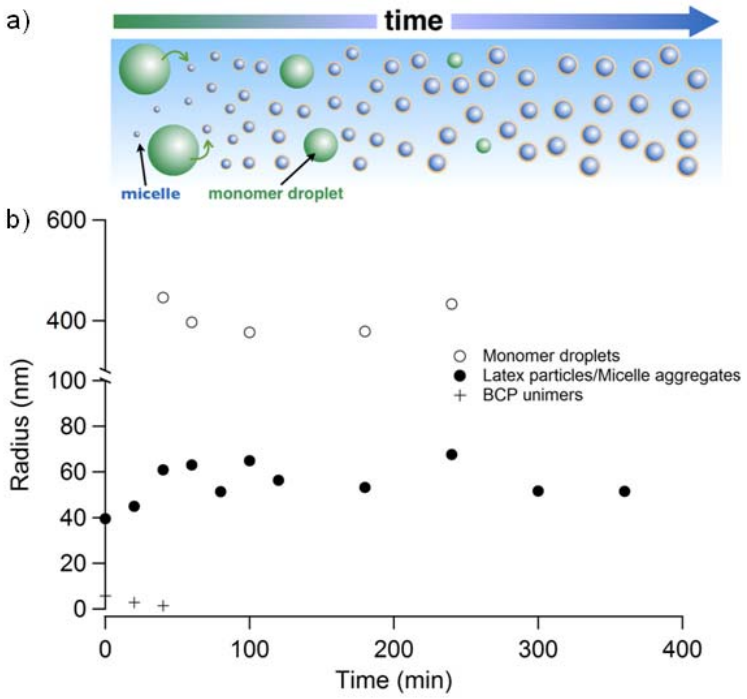

Figure 4. (a) Conceptual illustration of particle formation over time and (b) dynamic light scattering of particle formation over the course of an emulsion polymerization.

BCPs with varying levels of AGE in the hydrophilic block were synthesized to maximize reactive functionality while control was maintained over particle formation. Because **M3** exerted the greatest synthetic control over particle size, **M1** and **M5** were synthesized to contain 1 and 5 mol% AGE to optimize the density of reactive functionality. Figure 5 shows representative SEM images of particles using 10 wt% **M1**, **M3**, and **M5**, respectively. Although **M1** produced larger particles than **M3** at that [BCP], both syntheses were well-controlled and led to relatively monodisperse latexes that crystallized into colloidal arrays. Particles synthesized with **M5** coagulated or were quite polydispersed. It is likely that the increased concentration of alkene groups on **M5** caused additional interparticle coupling that was not observed when lower AGE was incorporated.

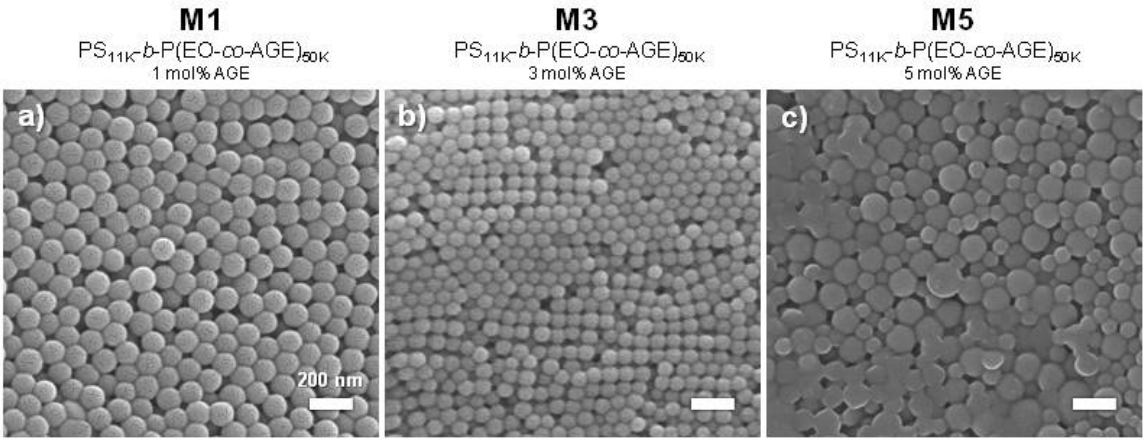

Figure 5. SEM images of particles synthesized with 10 wt% of BCP stabilizers with varying incorporations of AGE comonomer.

To capitalize on the potentially beneficial aspects of particles with a functional corona, verification of the presence of BCP on the periphery of the particles was required. Initially, particles with and without BCP were analyzed using XPS analysis, which elucidates the presence of elements as well as information about their bonding order within 1–10 nm of the surface. XPS analysis (Figure 6) indicated the presence of BCP within the first 10 nm of the surface, as evidenced by the C–O bond peak at 287 eV, which was absent in the bare PS latex. Angle-resolved XPS analysis allowed probing of different depths within the material, and a higher angle indicated shallower penetration of the x-ray beam. It was clear that there was no enrichment of ether-containing material within the first few nanometers (75° angle) over the larger depth profiled at 0°. Therefore, from the XPS analysis, we concluded that BCP was present within the particles and most likely, it resided on the surface. Fourier transform infrared spectroscopy (FTIR) was also used to monitor the incorporation of the BCP into the particles. Figure 7 shows an increase in absorbance by the ether groups, which is consistent with the increase in BCP loading in the emulsion polymerizations.

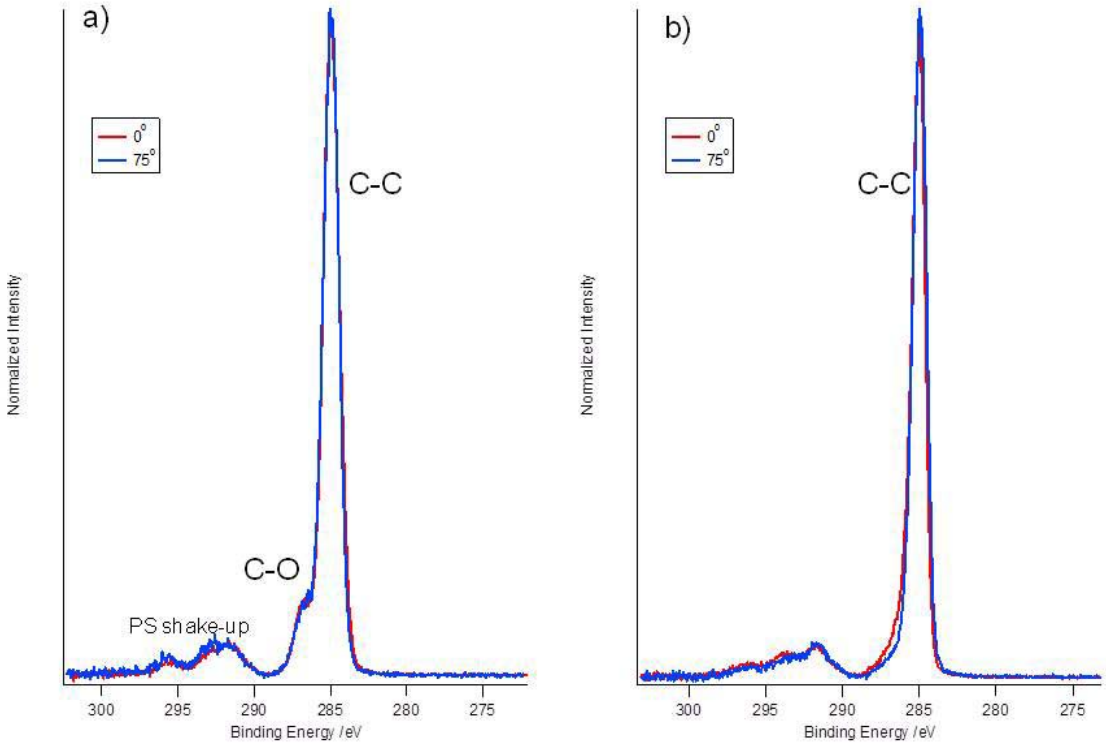

Figure 6. High-resolution carbon XPS spectra of (a) BCP-functional particles and (b) PS latexes.

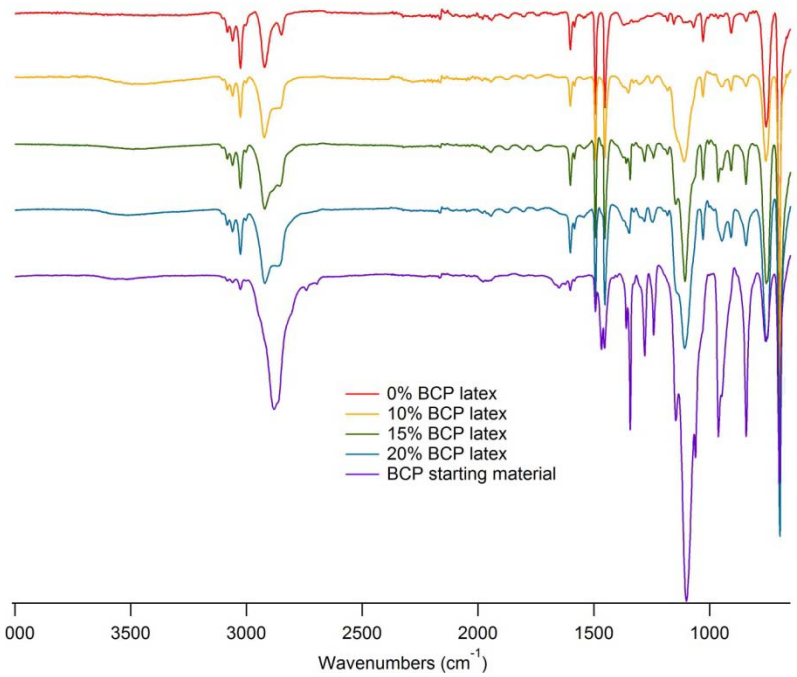

Figure 7. Overlay of FTIR spectra from particles with varying BCP incorporation.

3.4 THIOL-ENE FUNCTIONALIZED PARTICLES

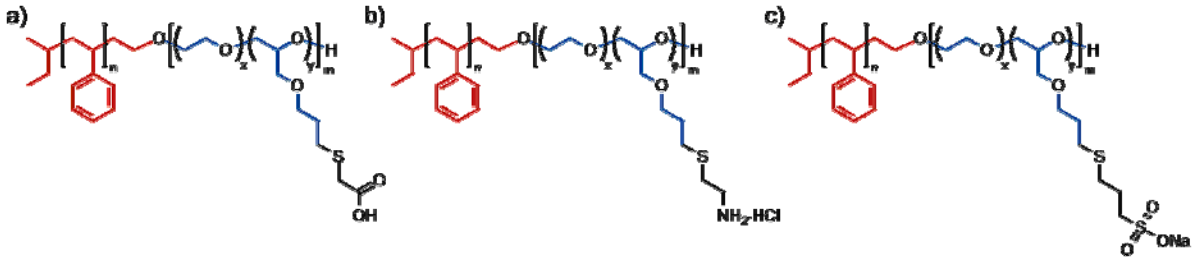

Figure 8. BCPs functionalized using thiol-ene click with (a) thioglycolic acid, (b) cysteamine hydrochloride, and (c) sodium 3-mercapto-1-propanesulfonate.

Functionalization of the BCPs was achieved using thiol-ene chemistry[29] to transform the allyl groups prior to polymerization. Groups that impart pH switchability to the resultant particles were selected. Commercially available thiols, including thioglycolic acid, cysteamine hydrochloride, and sodium 3-mercapto-1-propanesulfonate (Figure 8), were appended to the BCP using the photochemically-initiated thiol-ene reaction. Full conversion of the allyl groups was confirmed using ^{1}H NMR. Emulsion polymerization reaction conditions analogous to those used for the alkene-functional particles were employed. Particle diameters are shown in Table 4. Analogous to alkene-functional particles, sizes obtained by SEM were dramatically smaller than those measured by DLS for all functional particles. At neutral pH, all three samples were expected to be charged, and electrostatic repulsion caused the chains to be fully extended in the polymer corona, making them appear larger by DLS. Particles with carboxylic acid groups were much larger and more polydisperse than those prepared with the parent BCP. Conversely, sulfonate and amine-functional particles were markedly smaller than the alkene-functional particles of the same composition. Representative SEM images of the functional particles are shown in Figure 9.

Table 4. Properties of Functional Particle Samples

Functionality	**BCP used**	**Wt% BCP**	D_{DLS} **(nm)**[a]	D_{SEM} **(nm)**[b]
carboxylic acid	**M3**	15	270 ± 28	161 ± 51
amine	**M3**	15	128 ± 8	59 ± 8
sulfonate	**M3**	15	137 ± 6	60 ± 12

[a] Determined by DLS using Wyatt Dynamics software. Measured at pH 7.
[b] Determined by SEM using ImageJ software.

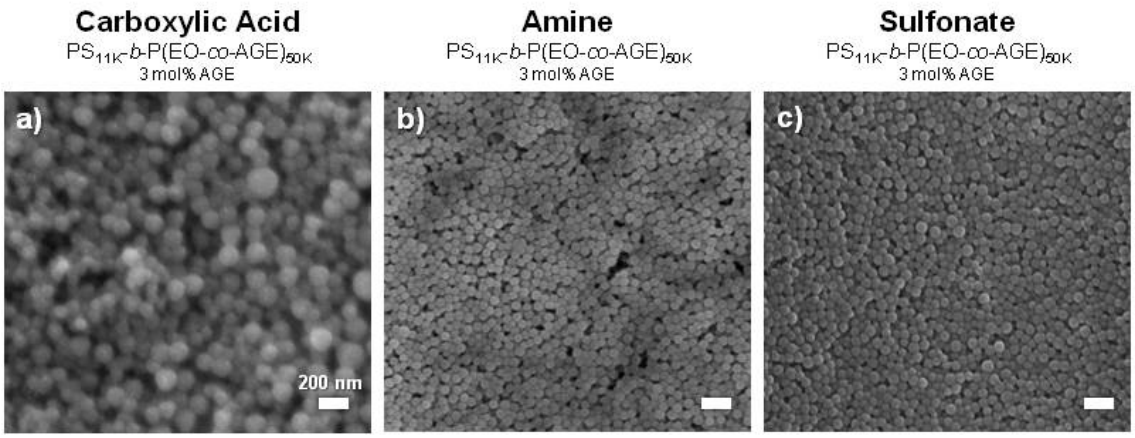

Figure 9. SEM images of particles synthesized with 15 wt% of functional BCP stabilizers.

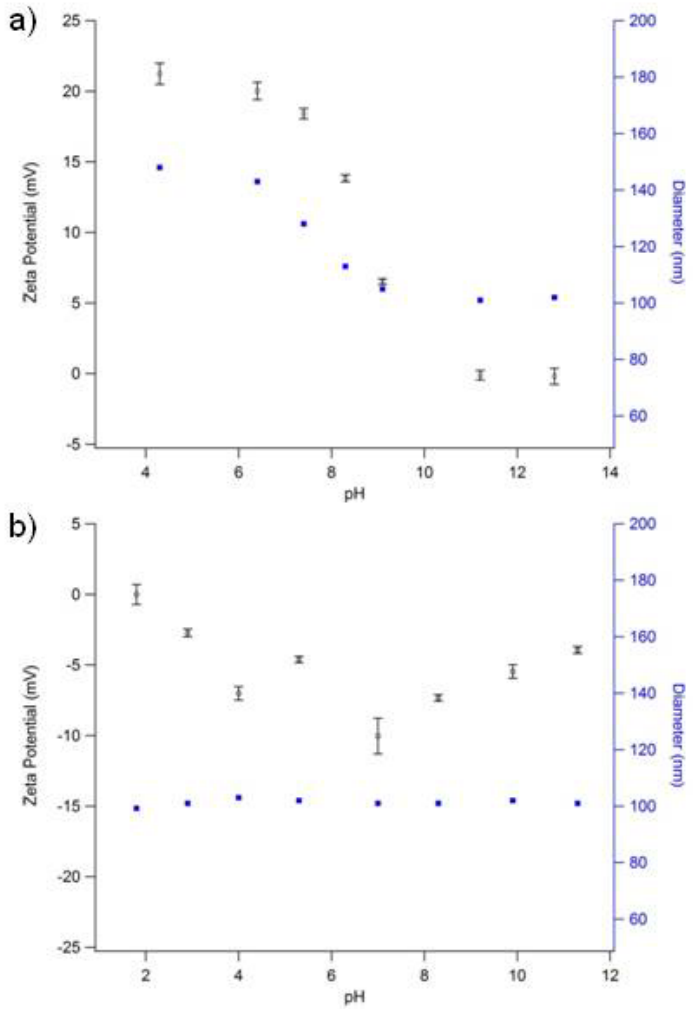

Figure 10. Zeta potential and diameter vs pH of alkene-functional (top) and ammonium-functional (bottom) particles.

The presence of ionizable groups on the functional particles caused them to exhibit pH switchability, which was probed by measuring their zeta potential. In an electrophoretic mobility measurement, particles having a surface charge migrate in solution according to the direction of an applied voltage potential. As shown in Figure 10, zeta potential and diameter were measured for ammonium particles at a pH values range. The particles were highly charged, with a large, positive zeta potential at pH values below the pK_a of ammonium. As the pH was increased, the particles became less charged, and zeta potential values approached zero at and above the pK_a of 8.3. Interestingly, the particle diameter exhibited a similar trend, with a decrease in size as the particles became more neutrally charged. This observation was explained by static repulsion of the chains at low pH where they were highly charged, followed by a relaxation of chains in the corona as the charges were neutralized. Particles functionalized with sulfonates and carbonates showed a similar, but opposite trend, as they were neutral at low pH and became more negatively charged at higher pH values. Alternatively, the alkene-functional particles, which have no ionizable character, showed little change in zeta potential with pH. Furthermore, the diameter of the particles remained constant throughout the pH range. The electrophoretic mobility of the particles supports our hypothesis that that polymer chains indeed extend into solution to stabilize the particles, and that the chains are anchored to the particles.

4. CONCLUSIONS

A functional amphiphilic BCP, PS-*b*-poly(EO-*co*-AGE), was successfully employed as a stabilizer in emulsion polymerization. We demonstrated control over the size of the particles by varying the amount of BCP incorporated into the particles, which yielded particles with low polydispersity. However, this control was primarily exerted at a narrow molecular weight. Smaller and larger BCPs demonstrated a loss of control, primarily because of steric stabilization factors. The inclusion of allyl groups within the hydrophilic portion of the BCP allowed for modification of a single polymer scaffold to create a library of particles with functional corona. Analysis of XPS and zeta potential measurements indicated that the functional corona resided at the periphery of the particles and extended into solution. We predict that the type of functionality at the corona will have important implications for the self-assembly of the particles into colloidal crystal assemblies and for advanced applications, which will be explored in future studies.

LITERATURE CITED

1. Wei, B.; Rogers, B. J.; Wirth, M. J. Slip flow in colloidal crystals for ultraefficient chromatography. *J. Am. Chem. Soc.* **2012,** *134* (26), 10780–10782.

2. Daniele, M. A.; Bandera, Y. P.; Sharma, D.; Rungta, P.; Roeder, R.; Sehorn, M. G.; Foulger, S. H. Substrate-baited nanoparticles: A catch and release strategy for enzyme recognition and harvesting. *Small* **2012,** *8* (13), 2083–2090.

3. Kim, S.-H.; Lee, S.; Yang, S.-M.; Yi, G.-R. Self-assembled colloidal structures for photonics. *NPG Asia Materials* **2011,** *3* (1), 25–33.

4. Muñoz-Bonilla, A.; Herk, A. M.; Heuts, J. P. A. Preparation of hairy particles and antifouling films using brush-type amphiphilic block copolymer surfactants in emulsion polymerization. *Macromolecules* **2010,** *43* (6), 2721–2731.

5. Muñoz-Bonilla, A.; Herk, A. M.; Heuts, J. P. A. Adding stimuli-responsive extensions to antifouling hairy particles. *Polym. Chem.* **2010,** *1* (5), 624.

6. Fakhrullin, R. F.; Lvov, Y. M. "Face-lifting" and "make-up" for microorganisms: Layer-by-layer polyelectrolyte nanocoating. *ACS Nano* **2012,** *6* (6), 4557–4564.

7. Lee, S.-H.; Hoshino, Y.; Randall, A.; Zeng, Z.; Baldi, P.; Doong, R.-a.; Shea, K. J. Engineered synthetic polymer nanoparticles as igg affinity ligands. *J. Am. Chem. Soc.* **2012,** *134* (38), 15765–15772.

8. Zakrevskyy, Y.; Richter, M.; Zakrevska, S.; Lomadze, N.; Klitzing, R.; Santer, S. Light-controlled reversible manipulation of microgel particle size using azobenzene-containing surfactant. *Adv. Funct. Mater.* **2012,** *22* (23), 5000–5009.

9. Zhang, Q.; Yu, G.; Wang, W.-J.; Yuan, H.; Li, B.-G.; Zhu, S. Preparation of n/co triggered reversibly coagulatable and redispersible latexes by emulsion polymerization of styrene with a reactive switchable surfactant. *Langmuir* **2012,** *28* (14), 5940–5946.

10. Pargen, S.; Willems, C.; Keul, H.; Pich, A.; Möller, M. Surfactant-free synthesis of polystyrene nanoparticles using oligoglycidol macromonomers. *Macromolecules* **2012,** *45* (3), 1230–1240.

11. Riess, G. Micellization of block copolymers. *Prog. Polym. Sci.* **2003,** *28* (7), 1107–1170.

12. Mura, J.-L.; Riess, G. Polymeric surfactants in latex technology - polystyrene-poly(ethylene oxide) block copolymers as stabilizers in emulsion polymerization. *Polym. Adv. Technol.* **1995,** *6* (7), 497–508.

13. Jialanella, G.; Firer, E.; Piirma, I. Synthesis of polystyrene-block-polyoxyethylene for use as a stabilizer in the emulsion polymerization of styrene. *J. Polym. Sci., Part A: Polym. Chem.* **1992,** *30* (9), 1925–1933.

14. Berger, M.; Richtering, W.; Mülhaupt, R. Use of poly (styrene)-block-poly (ethyleneoxide) as emulsifier in emulsion polymerization. *Polym. Bull.* **1994,** *33*, 521–528.

15. Riess, G.; Labbe, C. Block copolymers in emulsion and dispersion polymerization. *Macromol. Rapid Commun.* **2004,** *25* (2), 401–435.

16. Dimitriou, M. D.; Zhou, Z.; Yoo, H.-S.; Killops, K. L.; Finlay, J. A.; Cone, G.; Sundaram, H. S.; Lynd, N. A.; Barteau, K. P.; Campos, L. M.; Fischer, D. A.; Callow, M. E.; Callow, J. A.; Ober, C. K.; Hawker, C. J.; Kramer, E. J. A general approach to controlling the surface composition of poly(ethylene oxide)-based block copolymers for antifouling coatings. *Langmuir* **2011,** *27* (22), 13762–13772.

17. Lee, B.; Kade, M. J.; Chute, J. A.; Gupta, N.; Campos, L. M.; Fredrickson, G. H.; Kramer, E. J.; Lynd, N. A.; Hawker, C. J. Poly(allyl glycidyl ether)-a versatile and functional polyether platform. *J. Polym. Sci., Part A: Polym. Chem.* **2011,** *49* (20), 4498–4504.

18. Killops, K. L.; Campos, L. M.; Hawker, C. J. Robust, efficient, and orthogonal synthesis of dendrimers via thiol-ene "click" chemistry. *J. Am. Chem. Soc.* **2008,** *130* (15), 5062–5064.

19. Killops, K. L.; Gupta, N.; Dimitriou, M. D.; Lynd, N. A.; Jung, H.; Tran, H.; Bang, J.; Campos, L. M. Nanopatterning biomolecules by block copolymer self-assembly. *ACS Macro Letters* **2012,** *1* (6), 758–763.

20. Piirma, I. Polymeric surfactants. In *Surfactant science series 42*, Marcel Dekker: New York, 1992.

21. Garnier, S.; Laschewsky, A. New amphiphilic diblock copolymers: Surfactant properties and solubilization in their micelles. *Langmuir* **2006,** *22* (9), 4044–4053.

22. Wilhelm, M.; Zhao, C. L.; Wang, Y.; Xu, R.; Winnik, M. A.; Mura, J. L.; Riess, G.; Croucher, M. D. Poly(styrene-ethylene oxide) block copolymer micelle formation in water: A fluorescence probe study. *Macromolecules* **1991,** *24* (5), 1033–1040.

23. Xu, R.; Winnik, M. A.; Hallett, F. R.; Riess, G.; Croucher, M. D. Light-scattering study of the association behavior of styrene-ethylene oxide block copolymers in aqueous solution. *Macromolecules* **1991,** *24* (1), 87–93.

24. Khan, T. N.; Mobbs, R. H.; Price, C.; Quintana, J. R.; Stubbersfield, R. B. Synthesis and colloidal behaviour of a polystyrene-b-poly (ethylene oxide) block copolymer. *Eur. Polym. J.* **1987,** *23* (3), 191–194.

25. Winzor, C. L.; Mrázek, Z.; Winnik, M. A.; Croucher, M. D.; Riess, G. Stabilization of dispersion polymerization by poly(styrene-b-ethylene oxide) copolymers. *Eur. Polym. J.* **1994,** *30* (1), 121–128.

26. Xu, R.; Hu, Y.; Winnik, M. A.; Riess, G.; Croucher, M. D. Study of polystyrene-poly (ethylene oxide) block copolymer micelles in aqueous solution by size-exclusion chromatography. *J. Chromatogr.* **1991,** *547*, 434–438.

27. Gruijthuijsen, K.; Rufier, C.; Phou, T.; Obiols-Rabasa, M.; Stradner, A. Light and neutron scattering study of peg-oleate and its use in emulsion polymerization. *Langmuir* **2012,** *28* (28), 10381–10388.

28. Riess, G. Block copolymers as polymeric surfactants in latex and microlatex technology. *Colloids Surf., A* **1999,** *153*, 99–110.

29. Campos, L. M.; Killops, K. L.; Sakai, R.; Paulusse, J. M. J.; Damiron, D.; Drockenmuller, E.; Messmore, B. W.; Hawker, C. J. Development of thermal and photochemical strategies for thiol−ene click polymer functionalization. *Macromolecules* **2008,** *41* (19), 7063–7070.

Blank

ACRONYMS AND ABBREVIATIONS

AGE	allyl glycidyl ether
BCP	block copolymer
DLS	dynamic light scattering
DMF	dimethylformamide
DMSO	dimethyl sulfoxide
EO	ethylene oxide
FTIR	Fourier transform infrared spectroscopy
HLB	hydrophilic-lipophilic balance
M_n	number average molecular weight
NMR	nuclear magnetic resonance
PEO	poly(ethylene oxide)
pK_a	negative base10 logarithm of the acid dissociation constant of a solution
PS	polystyrene
PS-*b*-PEO	polystyrene-*b*-poly(ethylene oxide)
PS-*b*-P(EO-*co*-AGE)	polystyrene-*b*-poly(ethylene oxide-*co*-allyl glycidyl ether)
SEC	size exclusion chromatography
SEM	scanning electron microscopy
THF	tetrahydrofuran
XPS	x-ray photoelectron spectroscopy


EDGEWOOD CHEMICAL BIOLOGICAL CENTER
A U.S. Army RDECOM Laboratory